Research paper

On the azimuth angle characteristics of the blast wave from an underground magazine model (III) -Experiments on the effect of the internal length-to-diameter ratio-

Yuta Sugiyama*†, Kunihiko Wakabayashi*, Tomoharu Matsumura*, and Yoshio Nakayama*

*National Institute of Advanced Industrial Science and Technology (AIST),
Central 5, 1−1−1 Higashi, Tsukuba-shi, Ibaraki, 305−8565 JAPAN
Phone: +81−29−861−0552
†Corresponding author: yuta.sugiyama@aist.go.jp

Received: June 7, 2017 Accepted: October 5, 2017

Abstract

We conducted small-scale explosion experiments to assess the effect of the shape of an underground magazine both with and without a dike. The values of the internal length-to-diameter ratio L/D of the magazine model were 9 and 21, respectively, with the inner diameter fixed as 38.8 mm. The overpressures of the blast wave were measured using piezoelectric pressure sensors. A series of explosion experiments provided the azimuth angle characteristics of the peak overpressures of the blast wave from the exit. Increasing L/D led to a reduction in the peak overpressure. We discuss the applicability of an empirical formula proposed previously for $L/D = 3$ but now for varying L/D, which implies that the azimuth angle characteristics depend only on properly referenced data such as the peak overpressure in the exit direction. This gives the peak-overpressure distribution around an underground magazine with $3 \leq L/D \leq 21$.

Keywords: small-scale experiment, blast wave, azimuth angle characteristics, underground magazine, magazine shape

1. Introduction

Underground (shotgun design) magazines are regulated by the Explosive Control Act in Japan. The regulations say that the explosives safety quantity distance (ESQD) should be secured uniformly from the outside wall of the underground magazine to residential area. However, after an explosive is detonated in an underground magazine, the generated shock wave exits the underground magazine via the opening as a blast wave that exhibits the highest peak overpressure along the exit direction, and any increment in the azimuth angle from the exit direction results in a weakening of the blast wave. This requires proper regulation to be based on scientific evidence.

We have previously conducted small-scale explosion experiments[1] and numerical simulations[2] to determine the azimuth angle characteristics of the blast wave from an underground magazine model in cases with and without a dike. The internal length-to-diameter ratio of the magazine, L/D, was 3. In the experiments, reflection at the dike enhanced the blast wave behind the magazine, whereas diffraction weakened it ahead of the magazine near the dike. We proposed an empirical equation for the peak-overpressure distribution, which could properly estimate the blast-wave strength as a function of the azimuth angle after the blast wave had developed fully. The flow patterns predicted numerically showed that the dike prevented the detonation products from expanding along the exit direction. The isobaric distribution in the case of an underground magazine would be described as an ellipse with a constantly moving center.

Underground magazines have different values of L/D and loading density (the ratio of the stored mass of explosive to the volume of the magazine chamber)[3)−7)]. To estimate the peak-overpressure distribution in the case of an arbitrarily shaped underground magazine, we need to understand the effect of magazine shape on the blast-wave propagation.

Previous studies[4),8),9)] have indicated that only the peak

overpressure of the shock wave at the magazine exit determines the strength of the blast wave outside. One-dimensional shock-tube theory predicts that the shock wave weakens as it propagates. Therefore, a long tube attenuates the shock wave inside and the blast-wave outside the underground magazine and shortens the ESQD. In the present study, we experimentally investigate the blast-wave propagation around a small-scale underground magazine model to clarify the effects of L/D on the blast-wave strength in cases with and without a dike model.

2. Experimental details

2.1 Test explosive

The test explosive is the same one as used in a previous study, wherein the details are given[1]. A pressed pellet of 0.50 g made of pentaerythritol tetranitrate (PETN, 95 wt %) and carbon powder (5 wt%) is used as an explosive. Two pellets are glued together and used as a 1.00-g pellet. Our data, as well as those from previous papers[1),5),6),9)], incorporate a distance K [m kg$^{-1/3}$] that is scaled by the mass of the explosive, where 1 m kg$^{-1/3}$ corresponds to 100 mm. An electrical detonator with 100 mg of lead azide is glued to the top of the pellet.

2.2 Setup

In our previous study[1], we showed experimental results for the case of $L/D = 3$. To understand the effect of L/D on the blast-wave strength, experiments with $L/D = 9$ and 21 are conducted in the present paper. The experimental setup is similar to that in our previous study. Figure 1 shows schematics of the magazine, cover, exit, and dike for the model with $L/D = 9$ mounted on a steel plate; the inner diameter D is fixed as 38.8 mm, and the length L is 349.2 mm. In the case of $L/D = 21$, the lengths colored red are increased by 465.6 mm.

The magazine is modeled using a cylindrical steel pipe with a wall thickness of 6 mm. The height of the cover model is 129.2 mm. Because complex blast-wave reflections occur around the exit and dike model, a solid wall near the exit is required to obtain good experimental reproducibility. Therefore, the exit model is made of steel, as shown in Figure 1. We fill inside and between the exit model and the cover model with clay of density 2,230 kg m^{-3}. Because the acoustic impedance of clay is much larger than that of air, any energy absorption from the air to the clay can be neglected.

The center of the explosive is placed 20 mm from the end wall of the magazine model. The origin of the coordinates (x, y, z) is located at the exit of the magazine model on the steel plate, and the azimuth angle is defined in the counterclockwise direction from the $+x$ direction, as shown in Figure 1.

The blast-wave pressures are recorded using a digital waveform recorder (H-TECH Triple mode 30622) and piezoelectric pressure sensors (PCB 113B28, 100 mV psi^{-1}) that are situated in the +10°, 0°, and −10° directions as shown in Figure 1. The distances between the magazine exit and the pressure sensors on the ground are 400, 800, 1200, and 1600 mm; the corresponding scaled distances are $K = 4$, 8, 12, and 16 m kg$^{-1/3}$, respectively. The magazine model is set on a rotary table that changes the azimuth angle between the exit direction and the pressure sensors. Because the magazine model is symmetric about the x axis, the azimuth angle changes from 0° to 180° in intervals of 10°.

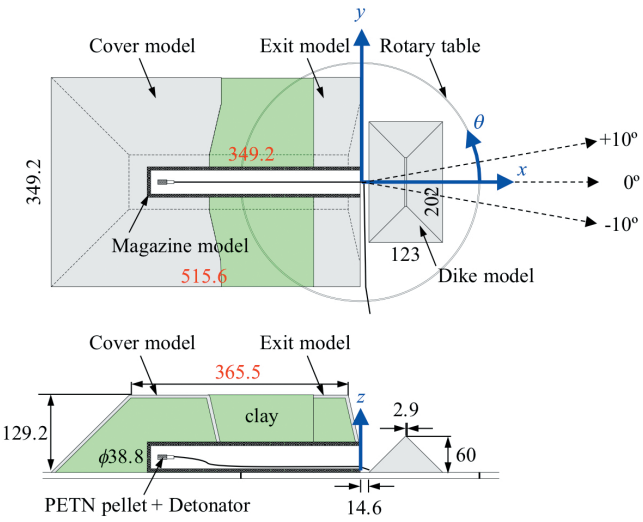

Figure 1 Schematics of the magazine, cover, exit, and dike model in the case of $L/D = 9$. In the case of $L/D = 21$, lengths colored red are increased by 465.6 mm.

In addition, we conduct surface-explosion experiments without any models to assess the enhancement and attenuation of the blast wave by the magazine and dike model. The explosive is placed vertically for a two-dimensional axisymmetric explosion, and the height between its center and the steel plate is 0.18 m kg$^{-1/3}$.

A series of explosion experiments is conducted to confirm the reproducibility of the peak overpressure and to provide the azimuth angle characteristics of the blast wave from the exit. Data in the present paper are values averaged over two or three experiments.

3. Results and discussion

The experiments give the pressure-time histories, which are interpolated using smooth cubic natural spline functions to obtain the peak overpressures. Figure 2 shows the relationship between peak overpressure and azimuth angle while varying L/D. The data shown in Figures 2(a–d) and 2(e–h) are for the cases with and without the dike, respectively.

Our previous studies[1),2)] and present experiments show a similar effect of the dike on the azimuth angle characteristics, as described below. The diffraction effect weakens the blast wave near the dike around 0°, but no longer appears at large scaled distances. Reflection off the dike enhances the blast wave behind the magazine, and the enhanced peak overpressure persists to large scaled distances. The peak overpressure around 180° increases locally. Because the cover model is symmetrical and has an angular shape as shown in Figure 1, the blast waves that propagate around it from the $+y$, $-y$, and $+z$ directions couple and strengthen.

Increasing L/D reduces the peak overpressures, as

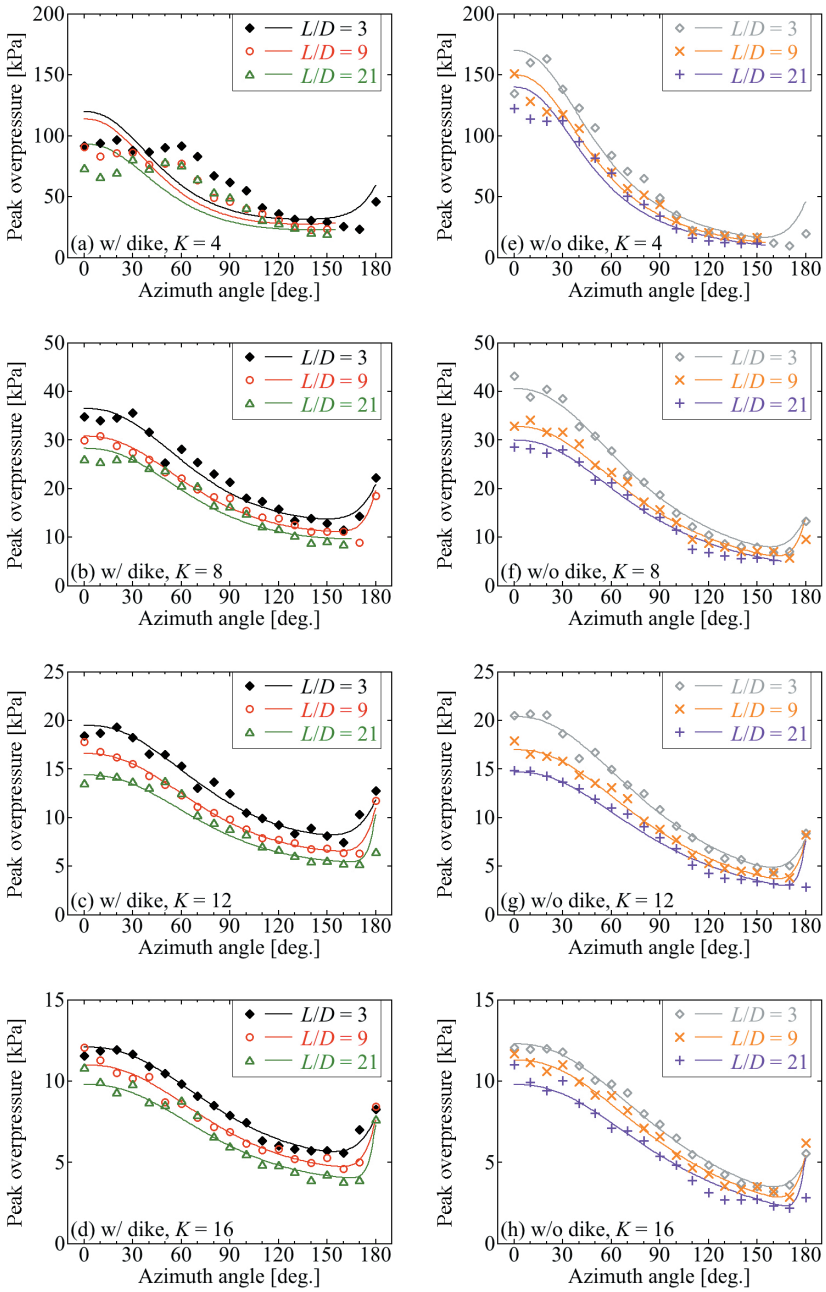

Figure 2 Azimuth angle characteristics of peak overpressure : (a-d) with dike ; (e-h) without dike.

shown in Figure 2 and Table 1. Table 1 denotes normalized and angle-averaged peak overpressures. The values are calculated by the following procedure. The data shown in Figure 2 are normalized with respect to those of $L/D = 3$ for each scaled distance, and the points between 0° and 180° are averaged for each scaled distance. The averaged values are listed in four columns in Table 1, where "Average" denotes the averaged values of the four scaled distances above.

One-dimensional shock-tube theory predicts that the shock wave should weaken as it propagates inside the tube. Therefore, a large value of L/D attenuates the shock wave inside and the blast wave outside the underground magazine. The cases of $L/D = 9$ and 21 show attenuations in peak overpressure of 15% and 25%, respectively, whereas the dike barely affects the attenuation ratio, as shown in Table 1.

In our previous study[1], we proposed Equation (1) to

Table 1 Normalized and angle-averaged peak overpressures. The values are calculated by the following procedure. The data in Figure 2 are normalized with respect to those of $L/D = 3$ for each scaled distance, and the points obtained between 0° and 180° are averaged for each scaled distance. The averaged values are listed in four columns, where "Average" denotes the averaged values of the four scaled distances above.

Scaled distance [m kg$^{-1/3}$]	$L/D = 9$		$L/D = 21$	
	w/ dike	w/o dike	w/ dike	w/o dike
4	0.84	0.89	0.78	0.73
8	0.88	0.85	0.76	0.72
12	0.83	0.84	0.72	0.72
16	0.89	0.91	0.79	0.74
Average	0.85	0.87	0.76	0.73

Table 2 Parameters for Equation (1).
(data with an asterisk are modified from Sugiyama et al.[1]).

dike	L/D	Scaled distance [m kg$^{-1/3}$]	$p_{peak}(0)$ [kPa]	a_1	n_1	a_2	n_2	a_3	n_3
w/	3[1)]	4	112.4*	55.9*	2.3	192	−21		−1.8
		8	36.5	82.1					
		12	19.5	92.0					
		16	12.1	102.3					
	9	4	113.8	57.7		185	−35	360	−1.9
		8	30.8	80.3					
		12	16.6	90.8					
		16	11.0	99.3					
	21	4	93.2	51.2		182	−60		−2.0
		8	28.3	82.0					
		12	14.4	89.4					
		16	9.8	99.3					
w/o	3[1)]	4	169.7*	55.9*		192	−21		
		8	40.6	82.1					
		12	20.4	92.0					
		16	12.3	102.3					
	9	4	140.0	57.7		185	−35	–	–
		8	32.8	80.3					
		12	17.0	90.8					
		16	11.3	99.3					
	21	4	124.2	51.2		182	−60		
		8	30.0	82.0					
		12	14.7	91.1					
		16	9.8	99.3					

consider separately the effects of blast-wave expansion (the first term), reflection of the blast waves from the $+y$, $-y$, and $+z$ sides at 180° (the second term), and reflection and diffraction off the dike (the third term when a dike is used) as

$$p_{peak}(\theta) = p_{peak}(0)\left\{\frac{1}{\left[1+\left(\frac{\theta}{a_1}\right)^{n_1}\right]}+\frac{1}{\left[1+\left(\frac{\theta}{a_2}\right)^{n_2}\right]}+\frac{1}{\left[1+\left(\frac{\theta}{a_3}\right)^{n_3}\right]}\right\}. \quad (1)$$

Parameters a_i and n_i denote the attenuation constants. Here we assume that $p_{peak}(0)$ is the primary parameter, and that a_1 changes according to the scaled distance and L/D, and is constant both with and without the dike; a_2, a_3, n_1, n_2, and n_3 depend only on L/D.

Table 2 lists the parameter values used in the present study. Data with an asterisk are modified from our previous study[1)]. The curves drawn in Figure 2 are from Equation (1). At 4 m kg$^{-1/3}$ with the dike, the blast wave is strongly disturbed by the dike, which is why the corresponding curves do not agree with the experimental data; hence, we exclude Figure 2(a) from our discussion of azimuth angle characteristics. Our proposed lines agree well with the experimental data after the blast wave has developed fully.

Table 2 gives some important indications, in particular, that n_1 and a_1 are independent of L/D at each scaled distance. This indicates that the blast-wave expansion from the exit can be normalized with respect to some reference datum. Our results support previous

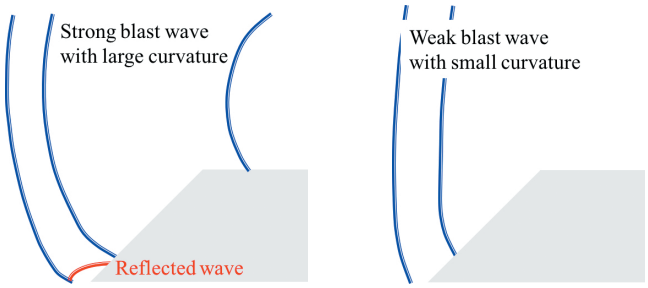

(a) small L/D (b) large L/D

Figure 3 Schematics of blast wave at $y = 0$ around cover model: (a) small L/D; (b) large L/D. The blast wave propagates from right to left in the schematics.

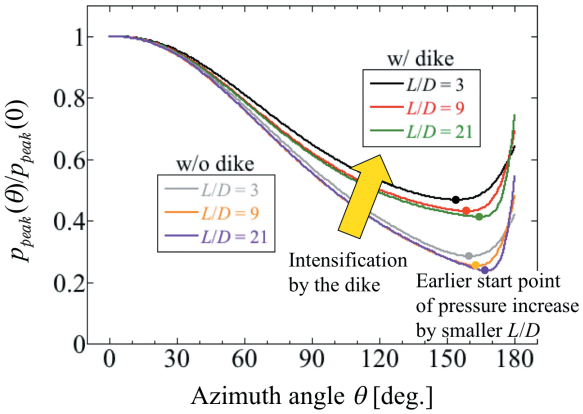

Figure 4 Azimuth angle characteristics of peak overpressure normalized with respect to $p_{peak}(0)$ at $K = 16$.

studies[4),8),9)] that indicated that only the peak overpressure of the shock wave at the exit can be used to normalize the peak overpressure outside. We will discuss the normalization of the azimuth angle characteristics with respect to the peak overpressure by $p_{peak}(0)$ as shown in Figure 4.

We review the values of n_1 and a_1 given in Table 2. When L/D is large enough, the peak overpressure is attenuated considerably with azimuth angle, as noted by Skjeltorp[3)] who used only a steel pipe and proposed $n_1 = 2.0$ and $a_1 = 56°$. We reason the following possible cause for this. In the case of large L/D, the one-dimensional shock wave inside the tube develops fully. The straight blast-wave expansion to the 0° direction gives the large attenuation of peak overpressure with increasing azimuth angle.

Parameters n_2 and a_2, which describe the reflection effect from the $+y$, $-y$, and $+z$ sides at 180° on the blast-wave enhancement, depend strongly on L/D at $K < 16$. The relationship between geometrical irregularity and blast-wave shape can explain this mechanism. Figure 3 shows the blast wave schematically at $y = 0$ behind the cover model at (a) small L/D and (b) large L/D. Because the blast wave expands hemispherically or semielliptically from the exit, its curvature decreases gradually. Because L/D is small, a strong blast wave with large curvature appears behind the cover model and reflects off the ground, as shown in Figure 3(a), resulting in strong reflection due to the small incident angle of the blast wave on the ground. As L/D becomes larger, the blast-wave expansion attenuates the peak overpressure at the cover

Table 3 Fitting parameters for Equation (3).

θ [deg.]	$L/D=3$				$L/D=9$				$L/D=21$			
	w/ dike		w/o dike		w/ dike		w/o dike		w/ dike		w/o dike	
	l	m	l	m	l	m	l	m	l	m	l	m
0	−1.489	2.868	−1.739	3.186	−1.456	2.822	−1.850	3.257	−1.421	2.709	−1.772	3.118
10	−1.486	2.870	−1.858	3.306	−1.445	2.790	−1.784	3.167	−1.377	2.650	−1.773	3.098
20	−1.497	2.890	−1.875	3.329	−1.512	2.839	−1.758	3.119	−1.453	2.722	−1.798	3.107
30	−1.460	2.839	−1.785	3.208	−1.542	2.854	−1.733	3.094	−1.545	2.827	−1.780	3.096
40	−1.501	2.846	−1.768	3.137	−1.465	2.754	−1.732	3.052	−1.541	2.787	−1.746	3.012
50	−1.534	2.852	−1.691	3.037	−1.572	2.820	−1.597	2.864	−1.588	2.840	−1.684	2.903
60	−1.610	2.921	−1.553	2.855	−1.597	2.827	−1.484	2.728	−1.559	2.786	−1.651	2.829
70	−1.616	2.880	−1.469	2.717	−1.529	2.707	−1.404	2.600	−1.550	2.726	−1.434	2.567
80	−1.476	2.712	−1.502	2.708	−1.391	2.526	−1.448	2.569	−1.520	2.626	−1.399	2.474
90	−1.476	2.677	−1.374	2.517	−1.384	2.496	−1.385	2.462	−1.535	2.613	−1.332	2.341
100	−1.450	2.596	−1.216	2.276	−1.354	2.415	−1.249	2.239	−1.452	2.488	−1.154	2.082
110	−1.335	2.427	−0.998	1.965	−1.342	2.362	−1.112	1.995	−1.337	2.296	−1.018	1.809
120	−1.280	2.337	−1.051	1.960	−1.222	2.229	−1.154	1.997	−1.288	2.228	−1.076	1.797
130	−1.221	2.235	−1.068	1.913	−1.168	2.132	−1.173	1.957	−1.263	2.155	−1.117	1.783
140	−1.189	2.210	−1.072	1.882	−1.115	2.040	−1.107	1.853	−1.196	2.033	−1.069	1.715
150	−1.169	2.168	−1.133	1.915	−1.085	2.021	−1.135	1.889	−1.127	1.977	−1.089	1.732
160	−1.100	2.064	−0.941	1.661	−1.280	2.198	−1.141	1.875	−1.165	1.983	−1.166	1.770
170	−0.843	1.895	−0.716	1.457	−0.837	1.705	−0.995	1.656	−1.018	1.818	−1.158	1.737
180	−1.232	2.425	−0.895	1.871	−1.139	2.298	−0.615	1.550	0.586	0.179	−0.061	0.526

model; smaller curvature gives weaker reflection, as shown in Figure 3(b).

Miura et al.[10] conducted numerical simulations of two-dimensional axisymmetric explosions with a dike and clarified the mitigating effects of the dike's configuration on the peak overpressure. They noted that the peak overpressure recovers behind the dike, and that its recovery rate with respect to distance decreases as the blast wave weakens. In the present study, as shown in Figure 3, the strong reflection gives faster peak-overpressure recovery and quick development of the reflected wave around 180°. Because the blast wave is strong enough, Equation (1) can properly estimate the peak overpressure even if the scaled distance is small. For example, in the case of $L/D=3$ with the dike, the reflected wave is fully developed at $4<K<8$, and the reflection effect properly estimates the experimental results of $K=8$, 12, and 16 as shown in Figure 2(b), (c), and (d), respectively. However, increasing L/D reduces the rate of peak-overpressure recovery and delays the generation of a fully developed reflected wave at 180°. The blast wave around the cover model in the case of $L/D=21$ without the dike is the weakest one in the present study, the reflected wave does not develop fully at $K=16$, and Equation (1) overestimates the peak overpressure at 180°, as shown in Figure 2 (h).

Parameters n_3 and a_3, which describe the effects of reflection and diffraction off the dike on the blast wave, are not strongly dependent on L/D. Smaller n_3 by increasing L/D denotes that the reflection effect at the dike becomes smaller with the weaker shock wave at the exit.

Finally, we summarize the azimuth angle characteristics of Equation (1) as shown in Figure 4, the vertical axis of which denotes the peak overpressure normalized with respect to p_{peak} (0) at $K=16$. This shows clearly that the dike intensifies the blast wave at $\theta \geq 60°$. Reflection of the blast waves that propagate around the cover model from $+y$, $-y$, and $+z$ at 180° could generate a triple point (like that observed previously in the flow field by numerical simulations[2]) that moves on the blast-wave surface. Because the triple point changes the peak overpressure before and after it, the start points of the pressure increase denote the positions of the triple point, as can be seen in the plots shown in Figure 4. As soon as the triple point is generated, it travels on the blast-wave surface in a circumferential direction and leaves from 180° as the blast wave expands. The start point then appears at a smaller angle in the case of smaller L/D.

To obtain the peak-overpressure distribution, the relationships between peak overpressure and scaled distance for each experimental condition are fitted as log-log plots. The obtained fitting parameters are m and n in the following equations:

$$X=\log K, \tag{2}$$

$$\log(p_{peak})=lX+m. \tag{3}$$

In our previous study[1] in the case of $L/D=3$, we obtained quadratics for the representative curves. In the present study, lines give better approximation than do quadratics. Hence, we use this linear approximation and again obtain the fitting parameters in the case of $L/D=3$. Table 3 presents the fitting parameters obtained in the present study.

Next, we discuss the attenuation and enhancement of the blast wave from the underground magazine. Figure 5

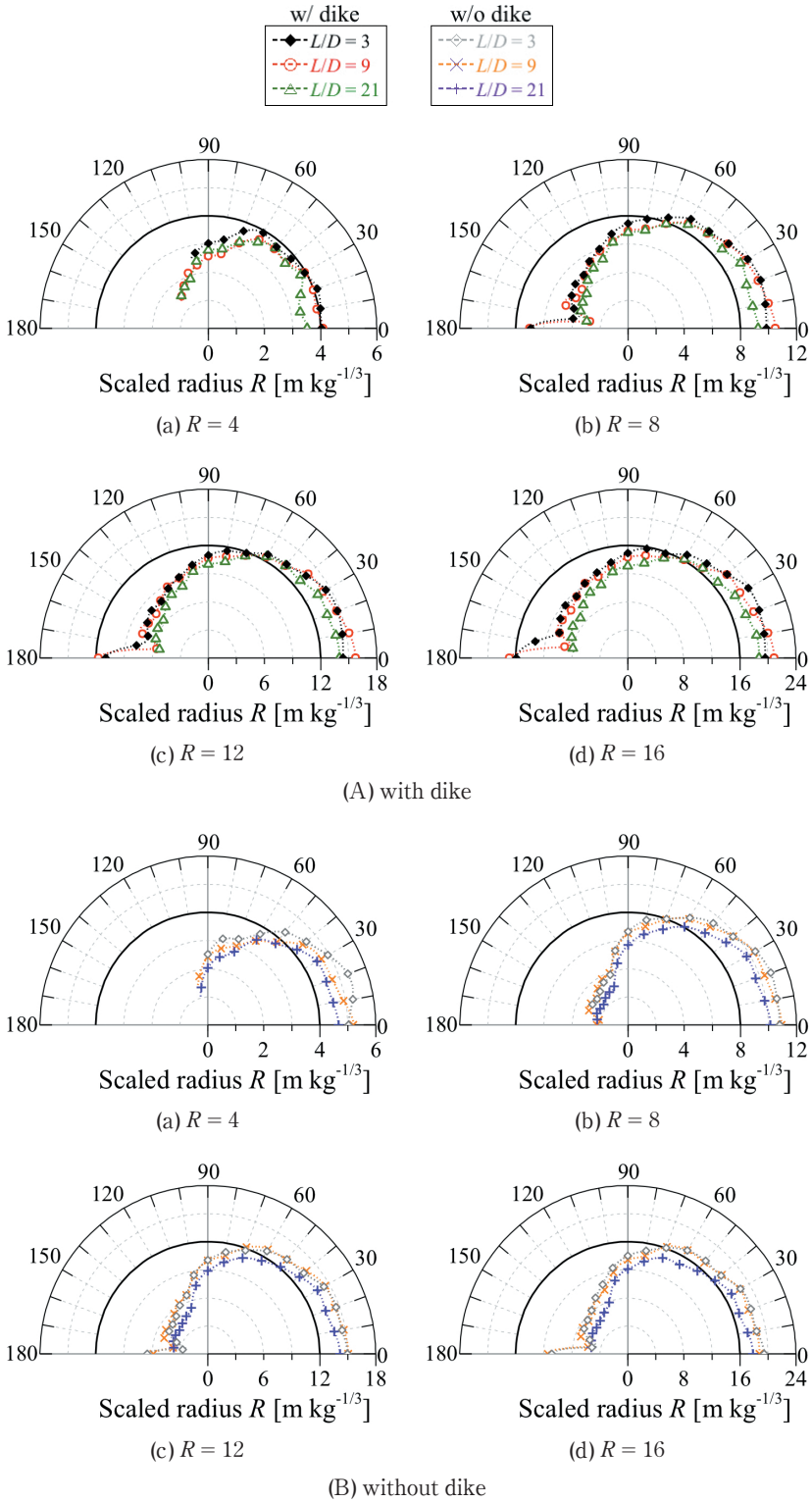

Figure 5 Isobaric lines of peak overpressure in cylindrical coordinates of scaled radius and azimuth angle. The peak overpressures correspond to those of the surface-explosion experiments at the scaled radius of (a) $R = 4$, (b) $R = 8$, (c) $R = 12$, and (d) $R = 16$. Black solid lines denote the isobaric lines of the surface-explosion experiments. Colored lines denote the isobaric lines (A) with the dike and (B) without the dike.

shows isobaric lines of the peak overpressure in cylindrical coordinates of scaled radius and azimuth angle in the case (A) with the dike and (B) without the dike. Because the surface explosion is conducted under two-dimensional axisymmetric conditions, its isobaric lines are circular. Black solid lines denote the isobaric lines of the surface-explosion experiments. The origin denotes the start point of the blast-wave expansion, which is the exit in the experiments with the underground magazine model and the ignition point in the surface-explosion experiments. The isobaric lines are obtained from Equation (3), and their peak overpressures correspond to those of the surface-explosion experiments at the scaled radius of (a) $R = 4$, (b) $R = 8$, (c) $R = 12$, and (d) $R = 16$. Increasing L/D leads to closer isobaric lines to the origin. The effect of L/D on the estimation of blast-wave strength against

azimuth angle could be used to determine the ESQD around an underground magazine.

4. Conclusions

We conducted small-scale explosion experiments to determine the azimuth angle characteristics of the blast wave from an underground magazine model in cases with and without a dike. The internal length-to-diameter ratio L/D was a parameter in the present study. When L/D increased, the peak overpressures were attenuated. We discussed the L/D dependency of the parameters by means of an empirical equation for the azimuth angle characteristics. The parameters were independent of L/D for the effects of the blast-wave expansion and the dike. Geometrical irregularity changed the parameters in the empirical equation. Increasing L/D led to closer isobaric lines to the origin. The effect of L/D on the estimation of blast-wave strength against azimuth angle could be used to determine the ESQD around an underground magazine.

Acknowledgment

This study was made possible by a Ministry of Economy, Trade, and Industry (METI) sponsored project entitled "Technical Standard for Explosion Mitigation of Explosives" in FY2016.

References

1) Y. Sugiyama, K. Wakabayashi, T. Matsumura, and Y. Nakayama, Sci. Tech. Energetic Materials, 77, 136–141 (2016).
2) Y. Sugiyama, K. Wakabayashi, T. Matsumura, and Y. Nakayama, Sci. Tech. Energetic Materials, 78, 49–54 (2017).
3) A. T. Skjeltorp, R. Jenssen, and A. Rinnan, Proc. Fifth International Symposium on Military Application of Blast Simulators, p. 6 : 7 : 1, Stockholm, May (1977).
4) C. N. Kingery, Technical Report BRL–TR–3012, June (1989).
5) Y. Nakayama, T. Matsumura, M. Iida, and M. Yoshida, Kayaku Gakkaishi (Sci. Tech. Energetic Materials), 62, 244–255 (2001). (in Japanese).
6) Y. Nakayama, D. Kim, K. Ishikawa, K. Wakabayashi, T. Matsumura, and M. Iida, Sci. Tech. Energetic Materials, 69, 123–128 (2008).
7) D. Kim and Y. Nakayama, Sci. Tech. Energetic Materials, 71, 88–91 (2010).
8) C. N. Kingery and E. J. Gion, BRL–TR–3132, Ballistics Research Laboratory (1990).
9) Y. Sugiyama, K. Wakabayashi, T. Matsumura, and Y. Nakayama, Sci. Tech. Energetic Materials, 76, 14–19 (2015).
10) H. Miura, A. Matsuo, and G. Tabuchi, Loss prev. Process Industries, 26, 329–337 (2013).